

Search for CP Violation in $D^0 \rightarrow K_S^0 \pi^+ \pi^-$

D. M. Asner and H. N. Nelson

University of California, Santa Barbara, California 93106

R. A. Briere, G. P. Chen, T. Ferguson, G. Tatishvili, and H. Vogel

Carnegie Mellon University, Pittsburgh, Pennsylvania 15213

N. E. Adam, J. P. Alexander, K. Berkelman, V. Boisvert, D. G. Cassel, J. E. Duboscq, K. M. Ecklund,
R. Ehrlich, R. S. Galik, L. Gibbons, B. Gittelman, S. W. Gray, D. L. Hartill, B. K. Heltsley, L. Hsu,
C. D. Jones, J. Kandaswamy, D. L. Kreinick, A. Magerkurth, H. Mahlke-Krüger, T. O. Meyer,
N. B. Mistry, J. R. Patterson, D. Peterson, J. Pivarski, S. J. Richichi, D. Riley, A. J. Sadoff,
H. Schwarthoff, M. R. Shepherd, J. G. Thayer, D. Urner, T. Wilksen, A. Warburton, and M. Weinberger

Cornell University, Ithaca, New York 14853

S. B. Athar, P. Avery, L. Breva-Newell, V. Potlia, H. Stoeck, and J. Yelton

University of Florida, Gainesville, Florida 32611

K. Benslama, C. Cawfield, B. I. Eisenstein, G. D. Gollin, I. Karliner,
N. Lowrey, C. Plager, C. Sedlack, M. Selen, J. J. Thaler, and J. Williams

University of Illinois, Urbana-Champaign, Illinois 61801

K. W. Edwards

*Carleton University, Ottawa, Ontario, Canada K1S 5B6
and the Institute of Particle Physics, Canada M5S 1A7*

D. Besson and X. Zhao

University of Kansas, Lawrence, Kansas 66045

S. Anderson, V. V. Frolov, D. T. Gong, Y. Kubota, S. Z. Li, R. Poling, A. Smith, C. J. Stepaniak, and J. Urheim

University of Minnesota, Minneapolis, Minnesota 55455

Z. Metreveli, K. K. Seth, A. Tomaradze, and P. Zweber

Northwestern University, Evanston, Illinois 60208

S. Ahmed, M. S. Alam, J. Ernst, L. Jian, M. Saleem, and F. Wappler

State University of New York at Albany, Albany, New York 12222

K. Arms, E. Eckhart, K. K. Gan, C. Gwon, K. Honscheid, D. Hufnagel,
H. Kagan, R. Kass, T. K. Pedlar, E. von Toerne, and M. M. Zoeller

Ohio State University, Columbus, Ohio 43210

H. Severini and P. Skubic

University of Oklahoma, Norman, Oklahoma 73019

S. A. Dytman, J. A. Mueller, S. Nam, and V. Savinov

University of Pittsburgh, Pittsburgh, Pennsylvania 15260

J. W. Hinson, J. Lee, D. H. Miller, V. Pavlunin, B. Sanghi, E. I. Shibata, and I. P. J. Shipsey

Purdue University, West Lafayette, Indiana 47907

D. Cronin-Hennessy, A. L. Lyon, C. S. Park, W. Park, J. B. Thayer, and E. H. Thorndike

University of Rochester, Rochester, New York 14627

T. E. Coan, Y. S. Gao, F. Liu, Y. Maravin, and R. Stroynowski

Southern Methodist University, Dallas, Texas 75275

M. Artuso, C. Boulahouache, S. Blusk, E. Dambasuren, O. Dorjkhaidav, N. Horwitz, G. C. Moneti,
R. Mountain, H. Muramatsu, R. Nandakumar, T. Skwarnicki, S. Stone, and J.C. Wang

Syracuse University, Syracuse, New York 13244

A. H. Mahmood

University of Texas - Pan American, Edinburg, Texas 78539

S. E. Csorna and I. Danko

Vanderbilt University, Nashville, Tennessee 37235

G. Bonvicini, D. Cinabro, M. Dubrovin, and S. McGee

Wayne State University, Detroit, Michigan 48202

A. Bornheim, E. Lipeles, S. P. Pappas, A. Shapiro, W. M. Sun, and A. J. Weinstein

California Institute of Technology, Pasadena, California 91125

(CLEO Collaboration)
(Dated: November 12, 2003)

We report on a search for CP violation in the decay of D^0 and \overline{D}^0 to $K_S^0\pi^+\pi^-$. The data come from an integrated luminosity of 9.0 fb^{-1} of e^+e^- collisions at $\sqrt{s} \approx 10 \text{ GeV}$ recorded with the CLEO II.V detector. The resonance substructure of this decay is well described by ten quasi-two-body decay channels plus a small non-resonant component. We observe no evidence for CP violation in the amplitudes that describe the decay $D^0 \rightarrow K_S^0\pi^+\pi^-$.

Phenomena that are not invariant with respect to charge conjugation and parity (CP) in strange [1, 2] and bottom [3, 4] mesons are the motivation for numerous current and future experiments. Standard Model (SM) predictions for the rate of CP violation in charm mesons are as large as 0.1% for $D^0 \rightarrow \pi^+\pi^-\pi^0$ [5, 6] but are considerably smaller, $\mathcal{O}(10^{-6})$, for $D^0 \rightarrow K_S^0\pi^+\pi^-$ where the dominant contribution is due to $K^0 - \overline{K}^0$ mixing [7]. The Dalitz technique [8, 9] allows increased sensitivity to CP violation by probing the decay amplitude rather than the decay rate. Observation of CP violation in $D^0 \rightarrow K_S^0\pi^+\pi^-$ at current experimental sensitivity would be strong evidence for non-SM processes. The decay $B^\pm \rightarrow DK^\pm$ followed by a multibody D^0 decay, such as $D^0 \rightarrow K_S^0\pi^+\pi^-$, may elucidate the origin of CP violation in the B sector [10].

We present the results of a search for CP violation in the amplitudes that contribute to $D^0 \rightarrow K_S^0\pi^+\pi^-$. Previous searches for direct CP violation [11, 12, 13, 14, 15] in the neutral charm meson system set limits of a few percent.

This analysis uses an integrated luminosity of 9.0 fb^{-1} of e^+e^- collisions at $\sqrt{s} \approx 10 \text{ GeV}$ provided by the Cornell Electron-positron Storage Ring (CESR). The data were taken with the CLEO II.V detector [16].

The event selection is identical to that used in our previous analysis of $D^0 \rightarrow K_S^0 \pi^+ \pi^-$ [17] which did not consider CP violation. We reconstruct candidates for the decay sequence $D^{*+} \rightarrow \pi_S^+ D^0$, $D^0 \rightarrow K_S^0 \pi^+ \pi^-$. The charge of the slow pion (π_S^+ or π_S^-) identifies the charm state as either D^0 or \bar{D}^0 . Consideration of charge conjugation is implied throughout this paper, unless otherwise stated.

We evaluate the energy released in the $D^{*+} \rightarrow \pi_S^+ D^0$ decay as $Q \equiv M^* - M - m_\pi$, where M^* is the reconstructed mass of the $\pi_S^+ K_S^0 \pi^+ \pi^-$ system, M is the reconstructed mass of the $K_S^0 \pi^+ \pi^-$ system, and m_π is the charged pion mass. We require the D^{*+} momentum p_{D^*} to exceed $2.0 \text{ GeV}/c$. We reconstruct $K_S^0 \rightarrow \pi^+ \pi^-$ with the requirement that the daughter pion tracks form a common vertex, in three dimensions, with a confidence level $> 10^{-6}$. Signal candidates pass the vertex requirement with 96% relative efficiency. Throughout this paper, relative efficiency is defined as the number of events in the data passing all requirements relative to the number of events when only the requirement under study is relaxed.

Our silicon vertex detector provides precise measurement of charged tracks in three dimensions [18]. We exploit the precision tracking by refitting the K_S^0 trajectory and π^\pm tracks with a requirement that they form a common vertex in three dimensions. We use the trajectory of the $K_S^0 \pi^+ \pi^-$ system and the position of the CESR luminous region to obtain the D^0 production point. We refit the π_S^+ track with a requirement that the trajectory intersect the D^0 production point. We require the confidence level of each refit exceed 10^{-4} . The signal candidates pass the D^0 production and decay vertex requirement with 85% and 91% relative efficiency, respectively.

We select 5,299 candidates within three standard deviations of the expected Q , M , and $m_{K_S^0}$. We compute σ_Q , σ_M and $\sigma_{m_{K_S^0}}$ from the trajectory reconstruction covariance matrices of the daughters of each D^{*+} candidate. The distributions of Q and M for the D^0 and \bar{D}^0 samples for our data are shown in Fig. 1. We find 2,579 D^0 and 2,720 \bar{D}^0 candidates corresponding to an asymmetry of $(-2.7 \pm 1.4 \pm 0.8)\%$, a 1.7σ effect.

In Fig. 2, we plot m_{RS}^2 vs $m_{\pi^+ \pi^-}^2$ where m_{RS} denotes the ‘right-sign’ and corresponds to $m_{K_S^0 \pi^-}$ for D^0 and $m_{K_S^0 \pi^+}$ for \bar{D}^0 . Similarly, m_{WS} denotes the ‘wrong-sign’ and corresponds to $m_{K_S^0 \pi^+}$ for D^0 and $m_{K_S^0 \pi^-}$ for \bar{D}^0 . We study our efficiency with a GEANT [19] based simulation of $e^+e^- \rightarrow c\bar{c}$ events in our detector with a luminosity corresponding to more than three times our data sample. We observe that our selection introduces distortions due to inefficiencies near the edge of phase space, and fit the efficiency to a two dimensional cubic polynomial $\mathcal{E}(m_{RS}^2, m_{\pi^+ \pi^-}^2)$. The reconstruction efficiencies for the D^0 and \bar{D}^0 over the Dalitz plot are consistent with each other and we take them to be equal; so $\mathcal{E}(m_{RS}^2, m_{\pi^+ \pi^-}^2) = \mathcal{E}(m_{WS}^2, m_{\pi^+ \pi^-}^2) = \mathcal{E}$.

Figure 1 shows that the background is small, but non-negligible, and we model our background as in Ref. [17]. To model the background contribution in the Dalitz distribution we consider those events in the data and MC that are in sidebands five to ten standard deviations from the signal in Q and M and within three in $m_{K_S^0}$. There are 235 (579) D^0 and 210 (572) \bar{D}^0 candidates in this selection in the data (MC), about four times the amount of background we estimate from the signal region. We constrain the invariant mass of the sideband candidates to the D^0 mass and compare with the background in our signal region from our simulation which also includes e^+e^- annihilations producing the lighter quarks. We note that the background from the simulation is dominated by random combinations of unrelated tracks. The simulation predicts that the background uniformly populates the allowed phase space. We model this contribution to the Dalitz distribution by fitting the D^0 mass constrained data sideband sample to a two dimensional cubic polynomial $\mathcal{B}(m_{RS}^2, m_{\pi^+ \pi^-}^2)$. All parameters except the constant are consistent with zero as predicted by simulation, so $\mathcal{B}(m_{RS}^2, m_{\pi^+ \pi^-}^2) = \mathcal{B}(m_{WS}^2, m_{\pi^+ \pi^-}^2) = \mathcal{B}$. The normalization of the uniform background in the data exceeds the simulation by $21 \pm 8\%$. Other possible contributions to the background, where $\pi\pi$ or $K\pi$ resonances combined with random tracks fake a D^0 and real D^0 decays combined with random soft pions of the wrong charge. The latter, called mistags, are especially dangerous to our search for CP violation as D^0 candidates are misidentified as \bar{D}^0 's. Since only two of the Dalitz parameters are independent [20], mistags populate the Dalitz distribution in a known way that depends on the shape of signal - namely we interchange assignment of m_{RS} and m_{WS} . When we analyze the Dalitz distribution, we allow a mistag fraction with an unconstrained contribution and we have looked for the contribution of a resonance, such as ρ^0 or $K^*(892)^-$, plus random tracks to the background in the data and conclude that any such contributions are negligible.

We parameterize the $K_S^0 \pi^+ \pi^-$ Dalitz distribution using the isobar model described in Ref. [9] where each resonance, j , has its own amplitude, a_j , and phase, δ_j . A second process, not necessarily of SM origin, could contribute to the j -th resonance. In general, we can express the amplitudes to the j -th quasi-two-body state as $(a_j e^{i(\delta_j \pm \phi_j)} \pm b_j e^{i(\delta_j \pm \phi_j)}) \mathcal{A}_j = a_j e^{i(\delta_j \pm \phi_j)} (1 \pm \frac{b_j}{a_j}) \mathcal{A}_j$, with ‘+’ for D^0 and ‘-’ for \bar{D}^0 and $\mathcal{A}_j = \mathcal{A}_j(m_{RS}^2, m_{\pi\pi}^2)$ is the amplitude for resonance j as described in Ref. [9]. Thus a_j and δ_j are explicitly CP conserving amplitudes and phases, b_j are explicitly CP violating amplitudes normalized by the corresponding CP conserving amplitude a_j , and ϕ_j are explicitly CP violating phases. In the absence of CP violation b_j and ϕ_j would be zero. The matrix elements \mathcal{M} and $\bar{\mathcal{M}}$ for the D^0 and \bar{D}^0 samples,

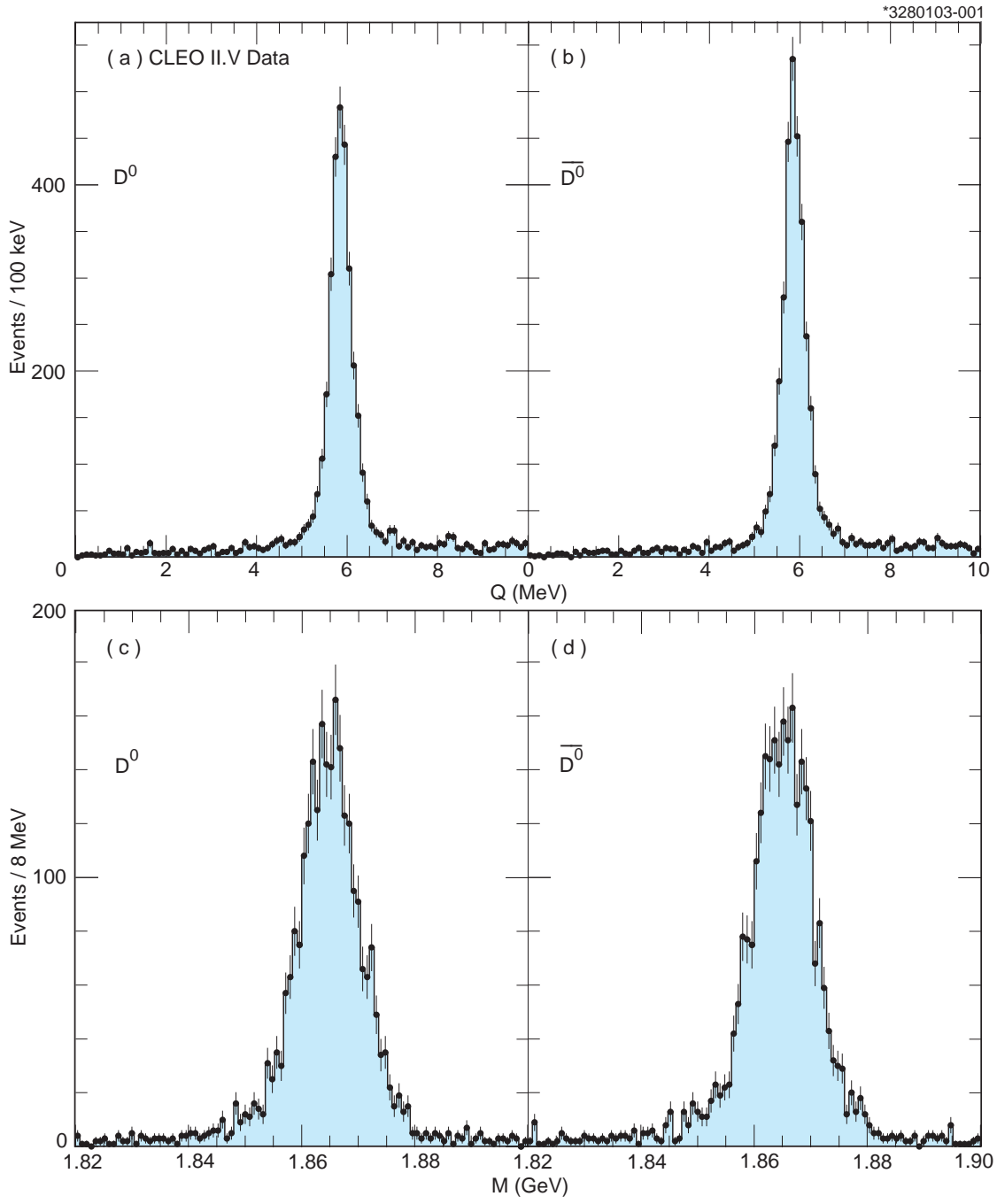


FIG. 1: Distribution of Q , (a) and (b), and M , (c) and (d), for the process D^0 and $\bar{D}^0 \rightarrow K_S^0 \pi^+ \pi^-$. The candidates pass all selection criteria discussed in the text.

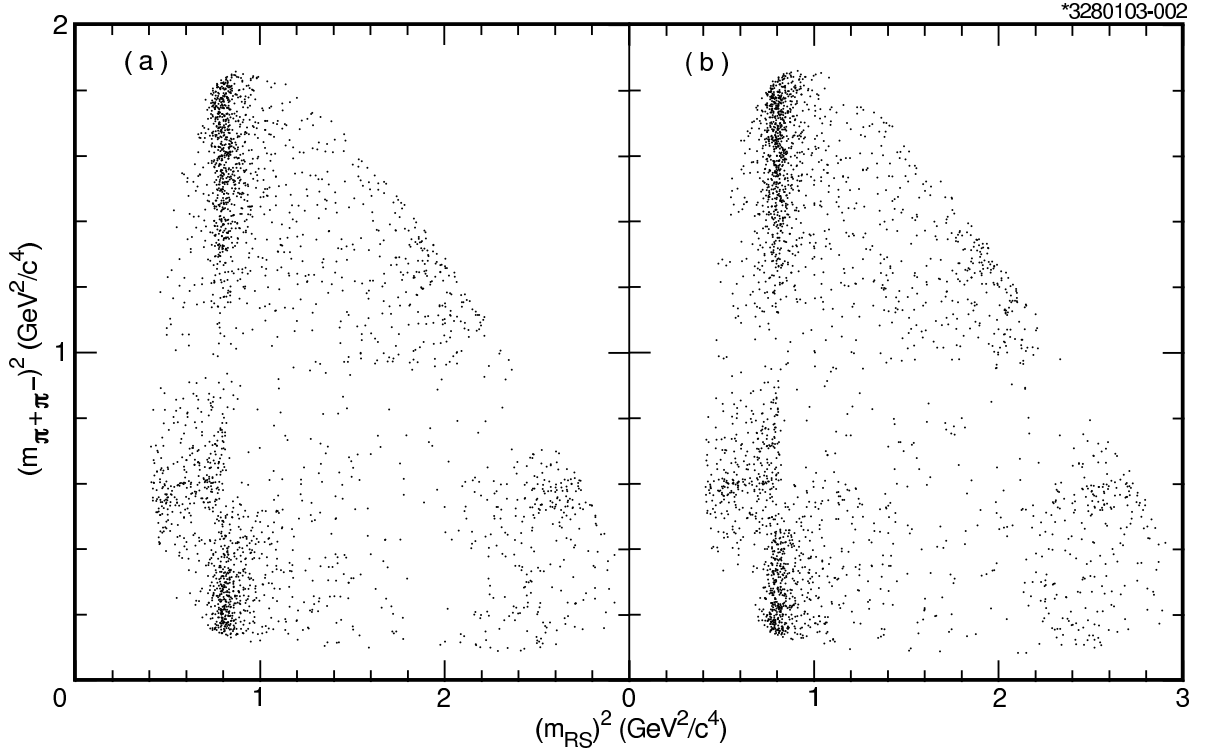


FIG. 2: Dalitz distribution for a) $D^0 \rightarrow K_S^0 \pi^+ \pi^-$ and b) $\bar{D}^0 \rightarrow K_S^0 \pi^+ \pi^-$ candidates passing all selection criteria discussed in Ref. [17]. The horizontal axis $(m_{RS})^2$ corresponds to $(m_{K_S^0 \pi^-})^2$ for D^0 and $(m_{K_S^0 \pi^+})^2$ for \bar{D}^0 .

respectively, are defined as

$$\mathcal{M} = a_0 e^{i\delta_0} + \sum_j a_j e^{i(\delta_j + \phi_j)} \left(1 + \frac{b_j}{a_j}\right) \mathcal{A}_j \quad (1)$$

$$\overline{\mathcal{M}} = a_0 e^{i\delta_0} + \sum_j a_j e^{i(\delta_j - \phi_j)} \left(1 - \frac{b_j}{a_j}\right) \mathcal{A}_j, \quad (2)$$

where a_0 and δ_0 parametrize the non-resonant amplitude, assumed to be CP conserving.

We perform an unbinned maximum likelihood fit which minimizes the function

$$\mathcal{F} = \left[\sum_{D^0} -2 \ln \mathcal{L} \right] + \left[\sum_{\bar{D}^0} -2 \ln \overline{\mathcal{L}} \right] + \left(\frac{F - F_0}{\sigma_F} \right)^2 \quad (3)$$

where

$$\mathcal{L} = T \left(F \frac{\mathcal{E} |\mathcal{M}(m_{RS}^2, m_{\pi\pi}^2)|^2}{\mathcal{N}} + (1-F) \frac{\mathcal{B}}{\mathcal{N}_{\text{background}}} \right) + (1-T) \left(F \frac{\mathcal{E} |\mathcal{M}(m_{WS}^2, m_{\pi\pi}^2)|^2}{\mathcal{N}} + (1-F) \frac{\mathcal{B}}{\mathcal{N}_{\text{background}}} \right) \quad (4)$$

$$\overline{\mathcal{L}} = T \left(F \frac{\mathcal{E} |\overline{\mathcal{M}}(m_{RS}^2, m_{\pi\pi}^2)|^2}{\mathcal{N}} + (1-F) \frac{\mathcal{B}}{\mathcal{N}_{\text{background}}} \right) + (1-T) \left(F \frac{\mathcal{E} |\overline{\mathcal{M}}(m_{WS}^2, m_{\pi\pi}^2)|^2}{\mathcal{N}} + (1-F) \frac{\mathcal{B}}{\mathcal{N}_{\text{background}}} \right) \quad (5)$$

and

$$\mathcal{N} \equiv \frac{1}{2} \left(\int \mathcal{E} |\mathcal{M}|^2 dm_{RS}^2 dm_{\pi\pi}^2 + \int \mathcal{E} |\overline{\mathcal{M}}|^2 dm_{RS}^2 dm_{\pi\pi}^2 \right) \quad (6)$$

$$\mathcal{N}_{\text{background}} \equiv \int \mathcal{B} dm_{RS}^2 dm_{\pi\pi}^2 \quad (7)$$

define the normalization of the D^0 , \overline{D}^0 , and background events. The signal fraction F_o and its error σ_F are determined from the fit to the combined D^0 and \overline{D}^0 mass spectra, shown in Fig. 1c) and d), to be 0.979 ± 0.015 . The signal fraction F and the mis-tag fraction $(1 - T)$ are consistent in the D^0 and \overline{D}^0 samples and we take them to be equal. The signal fraction F , the mistag fraction $(1 - T)$, and the parameters a_j, δ_j, b_j , and ϕ_j that describe the matrix elements \mathcal{M} and $\overline{\mathcal{M}}$ are determined by the Dalitz plot fit. We test the performance of our fit by generating 100 Monte Carlo samples from the results of our standard fit in Ref. [17]. The pull distributions of all fit parameters are consistent with unit Gaussian with zero mean indicating that the fit is not biased and that the errors are correctly computed.

We begin our search for CP violation from the results of our standard fit in Ref. [17] which clearly observed the ten modes, $(K^{*-}\pi^+, K_0^*(1430)^-\pi^+, K_2^*(1430)^-\pi^+, K^*(1680)^-\pi^+, K_S^0\rho, K_S^0\omega, K_S^0f_0(980), K_S^0f_2(1270), K_S^0f_0(1370)$, and the “wrong sign” $K^{*+}\pi^-$ plus a small non-resonant component. First, we fit the D^0 and \overline{D}^0 samples independently. The results of the D^0 and \overline{D}^0 fits are consistent with each other and with our CP conserving result [17]. Next, we fit the D^0 and \overline{D}^0 samples simultaneously. This fit has 42 free parameters, ten CP conserving amplitudes and ten CP conserving phases which are the same in the D^0 and \overline{D}^0 samples, ten CP violating amplitudes and ten CP violating phases which differ by a sign in the D^0 and \overline{D}^0 samples, plus two normalizations for the combinatoric and mistag backgrounds.

We report the CP conserving amplitude and phase, a_j and δ_j , in Table I. These results are consistent with our result in Ref. [17] in which CP conservation was assumed. We report the fractional CP violating amplitude and CP violating phase, b_j/a_j and ϕ_j in Table II. The three projections of the fit to the combined D^0 and \overline{D}^0 samples and the difference between the D^0 and \overline{D}^0 samples are shown in Fig. 3. We find the signal fraction F and mistag fraction $(1 - T)$ to be, $97.1 \pm 0.8\%$ and $0.0^{+0.7}_{-0.0}\%$, respectively. The confidence level of the fit, calculated directly from the likelihood function [9, 21], is 55%.

The amplitude a_j , on its own, is not a good estimator of the contribution of resonance a_j to the total rate. The width of a resonance, interference with other resonances and the allowed phase must be considered. The fit fraction (FF), formulated to encapsulate all these effects, is commonly defined as the integral of a single amplitude squared over the Dalitz plot (m_{RS}^2 vs $m_{\pi\pi}^2$) divided by the coherent sum of all amplitudes squared. We define the fit fraction as

$$FF_j = \frac{\int |(a_j + b_j)\mathcal{A}_j|^2 dm_{RS}^2 dm_{\pi\pi}^2}{\int |\mathcal{M}|^2 dm_{RS}^2 dm_{\pi\pi}^2} \quad (8)$$

$$\overline{FF}_j = \frac{\int |(a_j - b_j)\mathcal{A}_j|^2 dm_{RS}^2 dm_{\pi\pi}^2}{\int |\overline{\mathcal{M}}|^2 dm_{RS}^2 dm_{\pi\pi}^2} \quad (9)$$

for the D^0 and \overline{D}^0 samples, respectively. The CP conserving and CP violating fit fractions are defined as the sum and difference of the numerators of Eq. 8 and Eq. 9, respectively, divided by the sum of the denominators of Eq. 8 and Eq. 9.

The dominant constraint on CP violation is not due to limits on the CP violating amplitude squared but is due to the potential interference of a CP violating amplitude with a well determined CP conserving amplitude. We define the CP violating interference fraction (IF) as

$$IF_j = \frac{|\int \sum_k (2a_k e^{i\delta_k} \sin(\phi_k + \phi_j) \mathcal{A}_k) b_j \mathcal{A}_j dm_{RS}^2 dm_{\pi\pi}^2|}{\left(\int |\mathcal{M}|^2 dm_{RS}^2 dm_{\pi\pi}^2 + \int |\overline{\mathcal{M}}|^2 dm_{RS}^2 dm_{\pi\pi}^2 \right)} \quad (10)$$

where for the non-resonant component $\mathcal{A}_0 = 1$. The value of b_j determined by our fit is constrained by terms in the likelihood function proportional to $|b_j|^2$ and $a_k e^{+i\delta_k} b_j$ which are sensitive to both CP violation in the direct decay to a given submode and possible CP violation in interference with other modes, respectively. The CP violating fit fraction defined by Eqs. 8 and 9 is sensitive to CP violation in decay. The CP violating interference fractions of Eq. 10 sum over the contribution proportional to $a_k e^{+i\delta_k} b_j$ so are sensitive to CP violation in interference. The phases are important and allow the possibility of cancellation in this sum. This makes the IF a better representation of the impact of CP violation on the rate of decay than the CP violating FF. To quantify a fractional CP violation each decay channel, we define

$$A_{CP_j} = IF_j / FF_j, \quad (11)$$

where FF_j are the CP conserving fit fractions.

Note that the observation of CP violation with a significantly non-zero b_j/a_j or ϕ_j does not imply that *any* of the derived quantities, the CP violating FF_j , IF_j or A_{CP_j} will be non-zero. In particular, the CP violating effects that are locally non-zero can integrate to zero, thus IF_j and A_{CP_j} are more sensitive measures of CP violation than the CP violating fit fraction.

We use the full covariance matrix [22] from the fits to determine the errors on fit fractions and the CP violating interference fractions so that the assigned errors will properly include the correlated components of the errors on the amplitudes and phases. After each fit, the covariance matrix and final parameter values are used to generate 500 sample parameter sets. For each set, the fit fractions are calculated and recorded in histograms. The statistical error on the fit fractions is then extracted from the histograms. In Table I, we report the results for the CP conserving fit fractions, and the 95% upper limit for CP violating contributions are given in Table II. The fit fractions for the D^0 and \bar{D}^0 samples are given in Table III. An alternative measure of the rate of CP violation in a given submode is the asymmetry between the D^0 and \bar{D}^0 fit fractions, which are also given in Table III. The “Fit Fraction Asymmetry” is similar in sensitivity to A_{CP} defined by Eq. 11.

The common evaluation of the integrated CP asymmetry between normalized amplitudes squared across the Dalitz plot is sensitive to an asymmetry in shape between the D^0 and \bar{D}^0 samples and is defined as

$$A_{CP} = \int \frac{|\mathcal{M}|^2 - |\overline{\mathcal{M}}|^2}{|\mathcal{M}|^2 + |\overline{\mathcal{M}}|^2} dm_{RS}^2 dm_{\pi\pi}^2 / \int dm_{RS}^2 dm_{\pi\pi}^2. \quad (12)$$

We obtain $A_{CP} = -0.009 \pm 0.021^{+0.010+0.013}_{-0.043-0.037}$ where the errors are statistical, experimental systematic and modeling systematic, respectively.

We consider systematic uncertainties from experimental sources and from the decay model separately. Our general procedure is to change some aspect of our fit and interpret the change in the values of the amplitudes, phases and fit fractions in the non-standard fit relative to our nominal fit as an estimate of the systematic uncertainty. The impact of systematic uncertainties on the upper limit of the interference fraction, CP violating fit fraction and A_{CP} reported in Table II are estimated by recomputing the statistical error on these quantities with the covariance matrix of the non-standard fits using procedure described above. Contributions to the experimental systematic uncertainties arise from our model of the background, the efficiency, and biases due to experimental resolution. The background is modeled with a two dimensional cubic polynomial and the covariance matrix of the polynomial coefficients, both determined from a sideband. Our nominal fit fixes the coefficients of the background polynomial, and to estimate the systematic uncertainty on this background shape we perform a fit with the coefficients allowed to float constrained by the covariance matrix. Similarly we perform a fit with a uniform efficiency, rather than the nearly uniform efficiency determined from the simulation, as estimates of the systematic uncertainty due to the efficiency. We also perform fits where the background normalization and the efficiency of the D^0 and \bar{D}^0 samples are determined separately. We compute the overall normalization by evaluating the integrals in Eqs. 6 and 7 using Gaussian quadrature to interpolate between points on a finite grid across the Dalitz plot. To study the effect of the finite resolution our experiment has on the variables in the Dalitz plots we vary the granularity of the grid used to compute the overall normalization.

We change selection criteria in the analysis to test whether our simulation properly models the efficiency. We introduce a track momentum cut of 350 MeV/c to avoid the difficulty of modeling our low momentum tracking efficiency. We expand the signal region from three to six standard deviations in Q , M , and $m_{K_S^0}$, and increase the p_{D^*} cut from 2.0 to 3.0 GeV/c. These variations to the nominal fit are the largest contribution to our experimental systematic errors.

Contributions to the theoretical systematic uncertainties arise from our choices for the decay model for $D^0 \rightarrow K_S^0 \pi^+ \pi^-$. The standard value for the radius parameter [23] for the intermediate resonances and for the D^0 is 0.3 fm and 1 fm, respectively. We vary the radius parameter between zero and twice the standard value. Additionally, we allow the masses and widths for the intermediate resonances to vary within their known errors [20, 24, 25].

We consider the uncertainty arising from our choice of resonances included in the fit. We compared the result of our nominal fit to a series of fits where each of the resonances, σ or $f_0(600)$, $f_0(1500)$, $f_0(1710)$, $\rho(1450)$, $\rho(1700)$ were included one at a time. We also considered a fit including both the $f_0(600)$ and $f_0(1500)$ resonances. These variations to the nominal fit result in highly asymmetric variation in fit parameters and are the largest contribution to our modeling systematic error.

We take the maximum variation of the amplitudes, phases and fit fractions from the nominal result compared to the results in this series of fits as a measure of the experimental systematic and modeling systematic uncertainty.

In conclusion, we have analyzed the resonant substructure of the decay D^0 or $\bar{D}^0 \rightarrow K_S^0 \pi^+ \pi^-$ using the Dalitz-plot analysis technique and searched for CP violation in the amplitudes and phases of the ten clearly observed intermediate resonances. Our results, shown in Table II and Table III, are consistent with the absence of CP violation. We find the CP asymmetry in the fit fractions for each decay channel to be in the range $< (3.5 \text{ to } 28.4) \times 10^{-4}$ at the 95% confidence level. We find the CP asymmetry in the interference fractions for each decay channel to be in the range

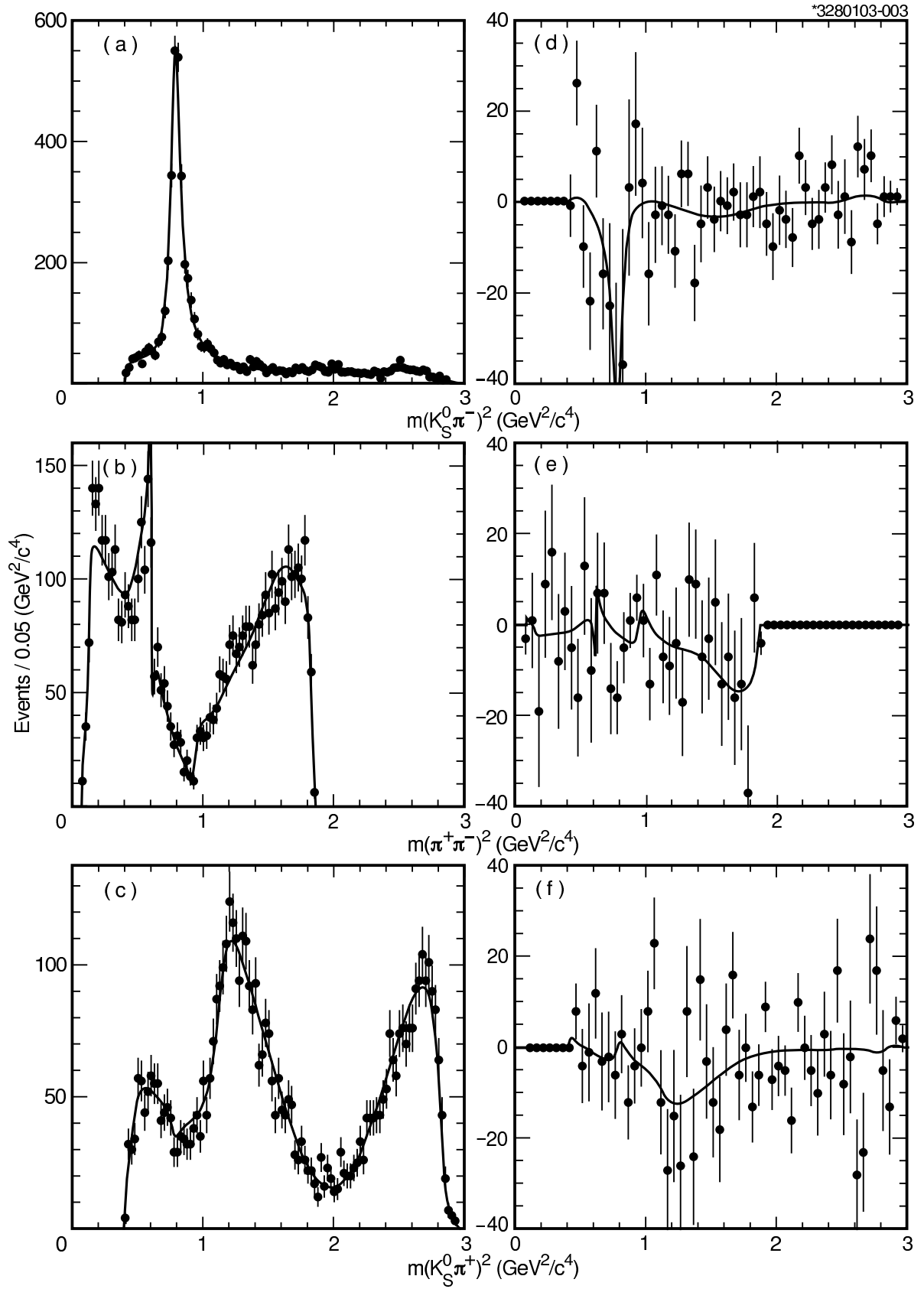


FIG. 3: Projections of the results of the fit described in the text to the $K_S^0 \pi^+ \pi^-$ Dalitz distribution showing both the fit (histogram) and the data (points). The combined D^0 and \bar{D}^0 samples are shown in (a), (b) and (c). The difference between the D^0 and \bar{D}^0 samples is shown in (d), (e) and (f).

$< (0.4 \text{ to } 22) \times 10^{-3}$ at the 95% confidence level. We find the ratio of the CP violating to CP conserving rate for each decay channel, to be in the range $< (0.3 \text{ to } 150)\%$ at the 95% confidence level. We find A_{CP} which is the asymmetry between normalized squared amplitudes integrated over the entire Dalitz plot to be $-0.009 \pm 0.021^{+0.010+0.013}_{-0.043-0.037}$.

Acknowledgment

We thank Eugene Golowich and Jon Rosner for valuable discussions. We gratefully acknowledge the effort of the CESR staff in providing us with excellent luminosity and running conditions. This work was supported by the National Science Foundation and the U.S. Department of Energy.

-
- [1] KTeV Collaboration, A. Alavi-Harati *et al.*, Phys. Rev. Lett. **83**, 22 (1999).
 - [2] NA48 Collaboration, V. Fanti *et al.*, Phys. Lett. B **465**, 335 (1999).
 - [3] BABAR Collaboration, B. Aubert *et al.*, Phys. Rev. Lett. **87**, 091801 (2001); BABAR Collaboration, B. Aubert *et al.*, Phys. Rev. Lett. **88**, 231801 (2002).
 - [4] Belle Collaboration, K. Abe *et al.* Phys. Rev. Lett. **87**, 091802 (2001); Belle Collaboration, K. Abe *et al.*, Phys. Rev. D **66**, 071102 (2002).
 - [5] F. Buccella, M. Lusignoli and A. Pugliese, Phys. Lett. B **379**, 249 (1996).
 - [6] P. Santorelli, arXiv:hep-ph/9608236.
 - [7] Z. Z. Xing, Phys. Lett. B **353**, 313 (1995) [Erratum-ibid. B **363**, 266 (1995)].
 - [8] R. H. Dalitz, Phil.Mag. 44, 1068 (1953).
 - [9] CLEO Collaboration, S. Kopp *et al.*, Phys. Rev. D **63**, 092001 (2001).
 - [10] A. Giri, Y. Grossman, A. Soffer and J. Zupan, Phys. Rev. D **68**, 054018 (2003).
 - [11] CLEO Collaboration, R. Godang *et al.*, Phys. Rev. Lett. **84**, 5038 (2000).
 - [12] E687 Collaboration, P. L. Frabetti *et al.*, Phys. Rev. D **50**, 2953 (1994).
 - [13] CLEO Collaboration, J. Bartelt *et al.*, Phys. Rev. D **52**, 4860 (1995); CLEO Collaboration, G. Bonvicini *et al.*, Phys. Rev. D **63**, 071101 (2001); CLEO Collaboration, G. Brandenburg *et al.*, Phys. Rev. Lett. **87**, 071802 (2001); CLEO Collaboration, S. E. Csorna *et al.*, Phys. Rev. D **65**, 092001 (2002).
 - [14] E791 Collaboration, E. M. Aitala *et al.*, Phys. Lett. B **421**, 405 (1998).
 - [15] FOCUS Collaboration, J. M. Link *et al.*, Phys. Lett. B **491**, 232 (2000) [Erratum-ibid. B **495**, 443 (2000)].
 - [16] CLEO Collaboration, Y. Kubota *et al.*, Nucl. Instrum. Methods Phys. Res. A **320**, 66 (1992); T.S. Hill, Nucl. Instrum. Methods Phys. Res. A **418**, 32 (1998).
 - [17] CLEO Collaboration, H. Muramatsu *et al.*, Phys. Rev. Lett. **89**, 251802 (2002) [Erratum-ibid. **90**, 059901 (2003)].
 - [18] CLEO Collaboration, G. Bonvicini *et al.*, Phys. Rev. Lett. **82**, 4586 (1999).
 - [19] GEANT manual, CERN Program Library Long Writeup W5013, Copyright CERN, Geneva, 1993.
 - [20] Particle Data Group, D.E. Groom *et al.*, Eur. Phys. J. **C 15**, 1 (2000).
 - [21] ARGUS Collaboration, H. Albecht *et al.*, Phys. Lett. B **308**, 435 (1993).
 - [22] See EPAPS Document No. [number will be inserted by publisher] for the full covariance matrix. A direct link to this document may be found in the online article's HTML reference section. The document may also be reached via the EPAPS homepage (<http://www.aip.org/pubservs/epaps.html>) or from <ftp.aip.org> in the directory /epaps/. See the EPAPS homepage for more information.
 - [23] J. Blatt and v. Weisskopf, *Theoretical Nuclear Physics*, New York: John Wiley & Sons (1952).
 - [24] E791 Collaboration, E. M. Aitala *et al.*, Phys. Rev. Lett. **86**, 765 (2001).
 - [25] A. Kirk, arXiv:hep-ph/0009168.

TABLE I: CP Conserving Parameters. Errors are statistical, experimental systematic and modeling systematic, respectively. The CP conserving fit fraction is computed from Eqs. 8 and 9 following the prescription described in the text.

Component	Amplitude (a_j)	Phase (δ_j) ($^\circ$)	Fit Fraction (%)
$K^*(892)^+\pi^- \times B(K^*(892)^+ \rightarrow K^0\pi^+)$	$(11 \pm 2_{-1}^{+4+2}) \times 10^{-2}$	$324 \pm 12_{-2-13}^{+9+6}$	$0.34 \pm 0.13_{-0.04-0.03}^{+0.35+0.06}$
$\bar{K}^0\rho^0$	1.0 (fixed)	0 (fixed)	$26.7 \pm 1.1_{-0.8-2.7}^{+0.7+0.5}$
$\bar{K}^0\omega \times B(\omega \rightarrow \pi^+\pi^-)$	$(40 \pm 5 \pm 2_{-1}^{+7}) \times 10^{-3}$	115_{-7-2}^{+6+4+3}	$0.81 \pm 0.19_{-0.08-0.06}^{+0.07+0.17}$
$K^*(892)^-\pi^+ \times B(K^*(892)^- \rightarrow \bar{K}^0\pi^-)$	$1.54 \pm 0.04_{-0.02-0.02}^{+0.01+0.11}$	$150 \pm 2 \pm 2$	$66.3 \pm 1.3_{-2.7-3.3}^{+0.7+2.3}$
$\bar{K}^0f_0(980) \times B(f_0(980) \rightarrow \pi^+\pi^-)$	$0.34 \pm 0.02_{-0.02}^{+0.05+0.01}$	$188 \pm 5_{-4-4}^{+7+9}$	$4.2 \pm 0.5_{-0.4}^{+1.1+0.2}$
$\bar{K}^0f_2(1270) \times B(f_2(1270) \rightarrow \pi^+\pi^-)$	$0.79 \pm 0.23_{-0.13-0.51}^{+0.27+0.39}$	$306_{-15-23-3}^{+13+7+54}$	$0.36 \pm 0.22_{-0.12-0.15}^{+0.31+0.08}$
$\bar{K}^0f_0(1370) \times B(f_0(1370) \rightarrow \pi^+\pi^-)$	$1.74 \pm 0.13_{-0.22-0.20}^{+0.23+0.10}$	$85 \pm 5_{-1-12}^{+5+2}$	$9.8 \pm 1.4_{-1.1-2.9}^{+2.4+1.1}$
$K_0^*(1430)^-\pi^+ \times B(K_0^*(1430)^- \rightarrow \bar{K}^0\pi^-)$	$1.93 \pm 0.11_{-0.17-0.09}^{+0.04+0.30}$	$1 \pm 5_{-4-14}^{+6+8}$	$7.2 \pm 0.7_{-1.1-0.7}^{+0.3+1.4}$
$K_2^*(1430)^-\pi^+ \times B(K_2^*(1430)^- \rightarrow \bar{K}^0\pi^-)$	$0.94_{-0.11-0.10-0.06}^{+0.12+0.13+0.00}$	$335_{-8-6-23}^{+9+0+4}$	$1.1 \pm 0.2_{-0.2-0.2}^{+0.3+0.4}$
$K^*(1680)^-\pi^+ \times B(K^*(1680)^- \rightarrow \bar{K}^0\pi^-)$	$5.49_{-0.65-0.94}^{+0.67+0.74} \pm 3.9$	$175 \pm 7_{-6-3}^{+11+16}$	$2.3 \pm 0.5_{-0.7-1.2}^{+0.6+0.3}$
$\bar{K}^0\pi^+\pi^-$ non-resonant	$0.93_{-0.31-0.17-0.53}^{+0.34+0.59+0.92}$	$343_{-16-23-17}^{+23+58+74}$	$0.7 \pm 0.7_{-0.2-0.6}^{+1.1+1.8}$

TABLE II: CP Violating Parameters. Errors are statistical, experimental systematic and modeling systematic, respectively. The interference fraction, CP violating fit fraction and A_{CP} , computed from Eq. 8-Eq. 11, following the prescription described in the text, include statistical and systematic effects.

Component	Ratio (b_j/a_j)	Phase (ϕ_j) ($^\circ$)	Interference Fraction	CP Violating Fit Fraction	$A_{CP}(\%)$
				(95% Upper Limits)	
$K^*(892)^+\pi^- \times B(K^*(892)^+ \rightarrow K^0\pi^+)$	$-0.12_{-0.22-0.15-0.03}^{+0.21+0.09+0.11}$	$6_{-22-35-4}^{+21+13+18}$	$< 3.0 \times 10^{-3}$	$< 7.8 \times 10^{-4}$	< 92
$\bar{K}^0\rho^0$	$0.001 \pm 0.022_{-0.009-0.011}^{+0.011+0.002}$	$-1_{-18-31-3}^{+16+9+21}$	$< 0.7 \times 10^{-3}$	$< 4.8 \times 10^{-4}$	< 0.3
$\bar{K}^0\omega \times B(\omega \rightarrow \pi^+\pi^-)$	$-0.14_{-0.11-0.01-0.02}^{+0.10+0.11+0.01}$	$-8_{-19-30-3}^{+17+8+20}$	$< 0.4 \times 10^{-3}$	$< 9.2 \times 10^{-4}$	< 4.5
$K^*(892)^-\pi^+ \times B(K^*(892)^- \rightarrow \bar{K}^0\pi^-)$	$-0.002 \pm 0.012_{-0.003-0.002}^{+0.008+0.002}$	$-3_{-18-30-3}^{+16+9+21}$	$< 2.1 \times 10^{-3}$	$< 3.5 \times 10^{-4}$	< 0.3
$\bar{K}^0f_0(980) \times B(f_0(980) \rightarrow \pi^+\pi^-)$	$-0.04 \pm 0.06_{-0.04-0.04}^{+0.13+0.00}$	$9_{-17-29-3}^{+16+10+20}$	$< 4.2 \times 10^{-3}$	$< 6.8 \times 10^{-4}$	< 10.4
$\bar{K}^0f_2(1270) \times B(f_2(1270) \rightarrow \pi^+\pi^-)$	$0.16_{-0.27-0.37-0.18}^{+0.28+0.15+0.11}$	$22_{-20-32-2}^{+19+12+20}$	$< 4.4 \times 10^{-3}$	$< 13.5 \times 10^{-4}$	< 150
$\bar{K}^0f_0(1370) \times B(f_0(1370) \rightarrow \pi^+\pi^-)$	$0.08_{-0.05-0.11-0.03}^{+0.06+0.01+0.06}$	$8_{-17-28-4}^{+15+10+20}$	$< 22 \times 10^{-3}$	$< 25.5 \times 10^{-4}$	< 21
$K_0^*(1430)^-\pi^+ \times B(K_0^*(1430)^- \rightarrow \bar{K}^0\pi^-)$	$-0.02 \pm 0.06_{-0.02-0.01}^{+0.04+0.00}$	$-3_{-19-36-2}^{+17+13+23}$	$< 9.1 \times 10^{-3}$	$< 9.0 \times 10^{-4}$	< 14
$K_2^*(1430)^-\pi^+ \times B(K_2^*(1430)^- \rightarrow \bar{K}^0\pi^-)$	$-0.05 \pm 0.12_{-0.14-0.00}^{+0.04+0.04}$	$3_{-18-31-2}^{+17+10+21}$	$< 2.2 \times 10^{-3}$	$< 6.5 \times 10^{-4}$	< 22
$K^*(1680)^-\pi^+ \times B(K^*(1680)^- \rightarrow \bar{K}^0\pi^-)$	$-0.20_{-0.27-0.22-0.01}^{+0.28+0.05+0.02}$	$-3_{-20-25-2}^{+19+20+27}$	$< 19 \times 10^{-3}$	$< 28.4 \times 10^{-4}$	< 92

TABLE III: D^0 and \bar{D}^0 Samples. Errors are statistical, experimental systematic and modeling systematic, respectively. The fit fraction is computed from Eqs. 8 and 9 following the prescription described in the text. The Fit Fraction Asymmetry is computed as the difference between the D^0 and \bar{D}^0 Fit Fractions divided by the sum.

Component	D^0 Fit Fraction (%)	\bar{D}^0 Fit Fraction (%)	Fit Fraction Asymmetry (%)
$K^*(892)^+\pi^- \times B(K^*(892)^+ \rightarrow K^0\pi^+)$	$0.27 \pm 0.20_{-0.11-0.03}^{+0.39+0.10}$	$0.41 \pm 0.21_{-0.00-0.05}^{+0.39+0.09}$	$-21 \pm 42_{-28-4}^{+17+22}$
$\bar{K}^0\rho^0$	$27.5 \pm 1.6_{-0.8-2.7}^{+1.4+0.4}$	$25.9 \pm 1.5_{-0.8-2.7}^{+0.5+0.7}$	$3.1 \pm 3.8_{-1.8-1.2}^{+2.7+0.4}$
$\bar{K}^0\omega \times B(\omega \rightarrow \pi^+\pi^-)$	$0.61 \pm 0.24_{-0.09-0.09}^{+0.32+0.15}$	$1.03 \pm 0.31_{-0.21-0.07}^{+0.10+0.19}$	$-26 \pm 24_{-2-4}^{+22+2}$
$K^*(892)^-\pi^+ \times B(K^*(892)^- \rightarrow \bar{K}^0\pi^-)$	$68.0 \pm 1.8_{-3.2-3.6}^{+1.1+4.6}$	$64.7 \pm 1.7_{-2.2-3.0}^{+0.3+0.8}$	$2.5 \pm 1.9_{-0.7-0.3}^{+1.5+2.9}$
$\bar{K}^0f_0(980) \times B(f_0(980) \rightarrow \pi^+\pi^-)$	$4.0 \pm 0.8_{-0.1-0.4}^{+1.1+0.2}$	$4.4 \pm 0.7_{-1.3}^{+1.1+0.2}$	$-4.7 \pm 11.0_{-7.4-4.8}^{+24.9+0.3}$
$\bar{K}^0f_2(1270) \times B(f_2(1270) \rightarrow \pi^+\pi^-)$	$0.49 \pm 0.41_{-0.24-0.29}^{+0.61+0.14}$	$0.24 \pm 0.23_{-0.03-0.09}^{+0.71+0.06}$	$34 \pm 51_{-71-34}^{+25+21}$
$\bar{K}^0f_0(1370) \times B(f_0(1370) \rightarrow \pi^+\pi^-)$	$11.7 \pm 1.9_{-4.2-2.3}^{+2.3+0.7}$	$8.2 \pm 1.7_{-0.5-3.1}^{+2.5+1.5}$	$18 \pm 10_{-21-6}^{+2+13}$
$K_0^*(1430)^-\pi^+ \times B(K_0^*(1430)^- \rightarrow \bar{K}^0\pi^-)$	$7.1 \pm 1.1_{-0.7-0.6}^{+0.9+1.5}$	$7.2 \pm 1.1_{-1.4-0.7}^{+0.4+1.2}$	$-0.2 \pm 11.3_{-4.9-1.0}^{+8.6+1.9}$
$K_2^*(1430)^-\pi^+ \times B(K_2^*(1430)^- \rightarrow \bar{K}^0\pi^-)$	$1.0 \pm 0.4 \pm 0.4_{-0.1}^{+0.5}$	$1.1 \pm 0.3_{-0.1-0.3}^{+0.5+0.4}$	$-7 \pm 25_{-26-1}^{+8+10}$
$K^*(1680)^-\pi^+ \times B(K^*(1680)^- \rightarrow \bar{K}^0\pi^-)$	$1.5 \pm 0.6_{-1.0-0.8}^{+0.6+0.3}$	$3.2 \pm 0.8_{-0.2-1.7}^{+0.7+0.3}$	$-36 \pm 19_{-35-1}^{+9+5}$